

NPS-61-84-004

# NAVAL POSTGRADUATE SCHOOL

## Monterey, California



SHORT PULSE LASER AND  
PLASMA SURFACE INTERACTIONS

F. Schwirzke  
//

2 April 1984

Approved for public release; distribution unlimited

Prepared for:

Chief of Naval Research, Arlington, VA 22217 and  
Naval Research Laboratory, Washington, DC 20375

FedDocs  
D 208.14/2  
NPS-61-84-004

U 202-1412:

NP-61-24-009

NAVAL POSTGRADUATE SCHOOL  
Monterey, California

Commodore R. H. Shumaker  
Superintendent

David A. Schradly  
Provost

The work reported herein was supported with funds provided by the Naval Research Laboratory, Washington, DC through work request N0017383WR30173.

Reproduction of all or part of this report is authorized.

This report was prepared by:

UNCLASSIFIED

 KELLY KNOX LIBRARY  
 NAVAL POSTGRADUATE SCHOOL  
 MONTEREY CA 93943-5101

SECURITY CLASSIFICATION OF THIS PAGE (When Data Entered)

REPORT DOCUMENTATION PAGE		READ INSTRUCTIONS BEFORE COMPLETING FORM
1. REPORT NUMBER NPS-61-84-004	2. GOVT ACCESSION NO.	3. RECIPIENT'S CATALOG NUMBER
4. TITLE (and Subtitle) Short-Pulse Laser and Plasma Surface Interactions	5. TYPE OF REPORT & PERIOD COVERED Technical Report	
	6. PERFORMING ORG. REPORT NUMBER	
7. AUTHOR(s) F. Schwirzke	8. CONTRACT OR GRANT NUMBER(s)	
9. PERFORMING ORGANIZATION NAME AND ADDRESS Naval Postgraduate School Monterey, CA 93943	10. PROGRAM ELEMENT, PROJECT, TASK AREA & WORK UNIT NUMBERS 62715H; 125RXB10 N0017383WR30173	
11. CONTROLLING OFFICE NAME AND ADDRESS Chief of Naval Research, Arlington, VA 22217 Naval Research Laboratory, Washington, DC 20375	12. REPORT DATE April 1984	
	13. NUMBER OF PAGES 16	
14. MONITORING AGENCY NAME & ADDRESS (if different from Controlling Office)	15. SECURITY CLASS. (of this report) Unclassified	
	15a. DECLASSIFICATION/DOWNGRADING SCHEDULE	
16. DISTRIBUTION STATEMENT (of this Report) Approved for public release; distribution unlimited		
17. DISTRIBUTION STATEMENT (of the abstract entered in Block 20, if different from Report)		
18. SUPPLEMENTARY NOTES		
19. KEY WORDS (Continue on reverse side if necessary and identify by block number) Short laser pulse Damage mechanism Laser-induced unipolar arcing Unipolar arc model		
20. ABSTRACT (Continue on reverse side if necessary and identify by block number) Unipolar arcing has been shown to be the primary plasma-surface interaction process when a laser produced plasma is in contact with a surface. Evidence of unipolar arcing was found on targets irradiated with neodymium laser pulses of 5 ns duration. The burn pattern of a defocused low irradiance laser pulse consists exclusively of unipolar arc craters. No other damage is observable.		

DD FORM 1473  
1 JAN 73EDITION OF 1 NOV 65 IS OBSOLETE  
S/N 0102-LF-014-6601

UNCLASSIFIED

SECURITY CLASSIFICATION OF THIS PAGE (When Data Entered)



## INTRODUCTION

High power laser beams interact with targets by a variety of thermal, impulse, and electrical effects. The laser heated plasma causes surface ablation by thermal evaporation, ion sputtering, and unipolar arcing. While the first two are purely thermal and mechanical effects, the last one, unipolar arcing, is an electrical plasma-surface interaction process which leads to crater formation.

Unipolar arcing occurs when a hot plasma of sufficiently high electron temperature interacts with a surface. Without any external voltage applied, many electrical micro-arcs burn between the surface and the plasma driven by local variations of the sheath potential with the wall acting as both the cathode and anode.

The existence of unipolar arcs has been verified with extensive experimental evidence on many tokamak surfaces<sup>1-5</sup>. The term unipolar arc was first coined by Robson and Thoneman<sup>6</sup> in 1958. They reported the results of experiments which physically demonstrated this unipolar arc process on a mercury electrode.

A laser-produced plasma was first used in 1979 to study surface damage due to unipolar arcing. Laser induced unipolar arcing represents the most damaging and non-uniform plasma-surface interaction process since the energy available in the plasma concentrates towards the cathode spots. Thus, local surface erosion is much more severe than it would be for uniform energy deposition. The ejection of plasma jets from the craters leads

to ripples in the critical density contour and small scale magnetic field generation around the jets. Filamentary plasma structures surrounded by strong magnetic fields have been observed<sup>8</sup> on laser irradiated spherical targets for 1.5 ns Nd pulses at intensities of  $10^{12}$ - $10^{14}$  W/cm<sup>2</sup>.

Previous experiments using a 25 ns FWHM Korad 1500 Nd-laser showed that unipolar arcing is the primary plasma-surface interaction process when a laser produced plasma is in contact with the target surface.<sup>9</sup> The onset of arc damage is coincident with the onset of plasma formation. Never was there a plasma evident without attendant unipolar arc craters. At low irradiance there was no other laser damage (like melting) observed. All damage was in the form of unipolar arc damage. Since the scale lengths are very small, typically 1  $\mu$ m for the cathode spot, and the electrons provide the current flow, unipolar arcing should be considered as a fast evolving process with arcs forming within a nanosecond or less.

This paper reports on unipolar arc studies using the shorter pulse length of the Naval Research Laboratory neodymium laser which has a pulse width of 5 ns.

## UNIPOLAR ARC MODEL

The following unipolar arc model<sup>10,11</sup> elaborates upon the electric fields which are set up in the plasma and drive the arc. The condition of plasma quasi-neutrality,  $n_e = n_i$ , leads to the formation of a sheath wherever the plasma is in contact with a wall. The plasma potential is positive with respect to the wall. The magnitude of this sheath, or floating potential, is proportional to the electron temperature,  $T_e$ , depends weakly on the ion/electron mass ratio  $M_i/m_e$ , and is independent of the plasma density,

$$V_f = (kT_e/2e) \ln(M_i/2\pi m_e) \quad (1)$$

The sheath width is proportional to the Debye shielding length

$$\lambda_D = (kT_e/e^2 4\pi n_e)^{1/2} \quad (2)$$

Hence, the sheath electric field which is normal to the surface and ignites the arc, depends on the plasma pressure as

$$|E_n| \approx \frac{V_f}{\lambda_D} = (n_e kT_e)^{1/2} \pi^{1/2} \ln(M_i/2\pi m_e) \quad (3)$$

Once ignited the high density plasma above the cathode spot is biased with respect to the surface via the cathode fall potential of the arc. The high density plasma dominates the surrounding

lower density background plasma. The increased plasma pressure above the cathode spot thus also leads to an electric field  $E_r$  in the radial direction, tangential to the surface, Figure 1.

$$E_r = - \frac{kT_e}{en_e} \frac{dn_e}{dr} + \frac{j}{\sigma} \quad (4)$$

Neglecting the  $j/\sigma$  term<sup>10</sup>, this radial field leads to a reduction of the plasma potential in a ring-like area surrounding the higher plasma pressure above the arc spot by

$$\Delta V(r) = \frac{kT_e}{e} \ln \frac{n_e(r)}{n_{e0}} \quad (5)$$

The ratio of the maximum plasma density  $n_e$  above the cathode spot to the unperturbed plasma density  $n_{e0}$  can easily be of the order  $(n_e/n_{e0}) \sim 10^3$  or larger<sup>11</sup>. The reduced sheath potential in this ring area allows more electrons from the high energy tail in the maxwellian distribution to reach the surface, this closing the current loop of the unipolar arc. In fact, equating  $\Delta V$  with the sheath's floating potential, eq (1)

$$\Delta V = V_f$$

$$\frac{kT_e}{e} \ln \frac{n_e}{n_{e0}} = \frac{kT_e}{2e} \ln \frac{Mi}{2\pi m_e}$$



we find that independent of the electron temperature the sheath potential approaches zero when

$$\left( \frac{n_e}{n_{e0}} = \frac{Mi}{2\pi m_e} \right)^{1/2}$$

In this case, the electron return current to the surface is determined by  $n_e$  and the electron thermal velocity. This electron saturation current is

$$i_s^- = \frac{en_e v_e}{4} A$$

where  $A$  is the return current area and  $v_e$  the electron thermal velocity.



## LASER-INDUCED UNIPOLAR ARCING

A plasma generated by a neodymium laser pulse was used to study unipolar arcing on stainless steel surfaces. To obtain a smooth surface, the target disks were metallographically polished with a final polishing slurry of  $0.05\ \mu\text{m}$   $\text{Al}_2\text{O}_3$ . After one laser shot, the damage on the polished surface was observed with an optical and a scanning electron microscope.

Laser induced unipolar arcing was studied at two basically different laser-power and plasma-dynamic conditions at high and low irradiance.

### 1. High Irradiance

A high power laser pulse of 75 Joule is focused onto the target. The laser produced plasma expands from the small focal spot over the target surface into areas which were not illuminated by the laser. The area damaged by the plasma is much larger than the laser focus area. The existence of unipolar arc craters in these areas proves that unipolar arcing is a plasma-surface interaction process, independent of the laser-plasma interaction processes, like self-focusing, filamentation, instability, etc. The laser just heats the electrons to a sufficiently high temperature.

Figure 2 shows a 12mm diameter SS 304 target disk after one laser shot with the laser impact crater (focal spot) at the center. The high temperature laser produced plasma expands radially over the surface, roughening it up in the process.

Further enlargement, about 3mm from the laser impact crater, shows a V-like wave pattern, Figure 3, as if the liquid metal was being pushed against a pylon. If not filled up by the liquid metal, many of the V-shaped waves show a hole at the center, Figure 4, indicating that the plasma jet emitted from the unipolar cathode crater served as pylon. Near the edge of the target, 5-6 mm away from the laser impact crater, the typical shape of single unipolar arc craters, on an otherwise undamaged surface, becomes recognizable, an outer crater rim of variable size with a cathode hole at the center, Figure 5. The diameter of the outer crater rim depends on the duration of the arc. The dense plasma over the cathode spots expands in radial direction, melting a surface layer. The location of the outer crater rim thus indicates how far the return current area has expanded during the limited burn time of the arc. Near the edge of the target, we find craters with a well developed cathode hole and the crater rim formation just barely beginning, Figure 6.

## 2. Low Irradiance

A low power, defocused laser pulse is used to illuminate the target. Laser intensity variations over the beam cross section cause a burn pattern by breakdown and arcing in areas where the power density was sufficiently high. The area damaged by the plasma is smaller than the laser illuminated area.

Figure 7 shows a target which was placed 21 cm from the focal spot towards the focusing lens with a focal length of 110 cm. The laser beam cross section is larger than the target disk. The laser energy was reduced to 6 Joule. The burn pattern consists

of interference rings. Figure 8 shows a 100X enlargement of one of the rings with an optical microscope. Further enlargement shows that the pattern consists of single craters, Figure 9, 10, 11, with various sizes of the outer crater rim. Small cathode holes have a diameter of about  $0.7 \mu\text{m}$  which is smaller than the wave length of the Nd laser,  $\lambda = 1.06 \mu\text{m}$ .

A review of the target surface reveals that the damage is not evenly distributed. Besides the severe deformation caused by arcing, there is no other direct laser damage (like uniform surface melting) observable. All damage is in the form of arc damage. Obviously, the plasma manages to concentrate the laser-plasma energy available within the inference ring into the small cathode spots which have diameters  $d \sim \lambda$ .

### CONCLUSIONS

The experimental results show that unipolar arcing is the primary laser plasma-surface interaction mechanism for a 5 ns laser pulse which leads to a very non-uniform energy deposition on the ablation surface because unipolar arcing concentrates the available laser-plasma energy towards the cathode spot.

## ACKNOWLEDGEMENTS

This work was supported by the Naval Research Laboratory.

## REFERENCES

1. G. M. McCracken, J. Nucl. Mater. 93/94, 3 (1980).
2. R. E. Clausing, L. C. Emerson and L. E. Heatherly, J. Nucl. Mater. 93/94, 150 (1980).
3. G. M. McCracken and D. H. J. Goodall, Nucl. Fusion 18, 537 (1978).
4. S. A. Cohen, H. F. Dylla, S. M. Rossnagel, S. T. Picraux and C. W. Magee, J. Nucl. Mater. 76/77, 459 (1978).
5. P. Staib and G. Staudenmaier, J. Nucl. Mater. 76/77, 78 (1978).
6. A. E. Robson and P. C. Thonemann, Proc. Phys. Soc. 73, 508 (1959).
7. F. Schwirzke and R. J. Taylor, J. Nucl. Mater. 93/94, 780 (1980).
8. O. Willi and P. T. Rumsby, Optics Communications, 37, 45 (1981).
9. F. Schwirzke, M. H. Beelby and H. G. Ulrich, "Basic Mechanisms that Lead to Laser Target Damage", Naval Postgraduate School Report NPS-61-82-002 (1981).
10. F. Schwirzke, "Unipolar Arcing, A Basic Laser Damage Mechanism", Naval Postgraduate School Report, NPS-61-83-008 (1983).
11. F. Schwirzke, "Laser Induced Unipolar Arcing", Laser Interaction and Related Plasma Phenomena, H. Hora and G. M. Miley, Editors, Volume 6, p. 335-352, (1984), Plenum Publishing Corporation.

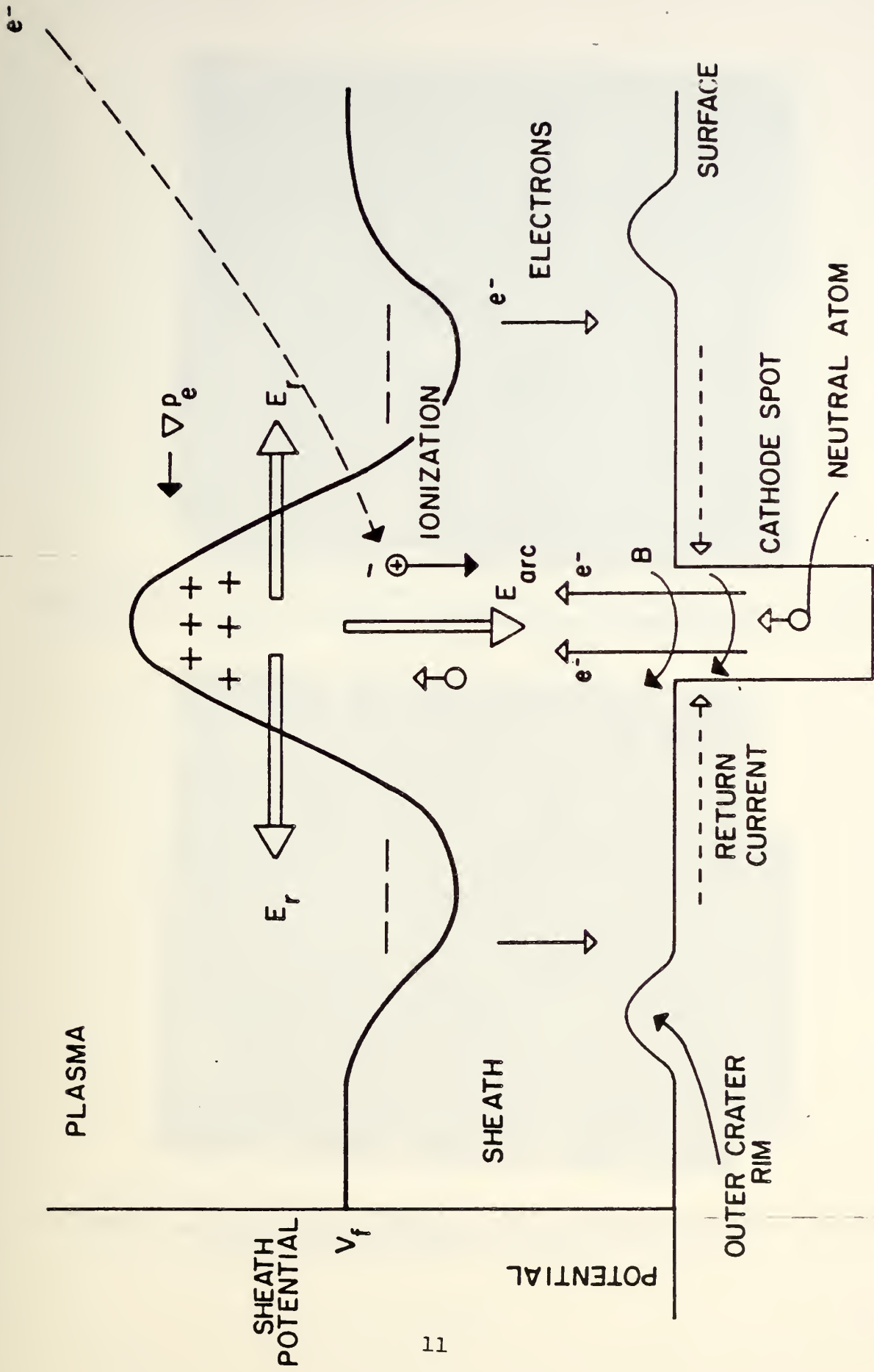


Figure 1. UNIPOLAR ARC MODEL

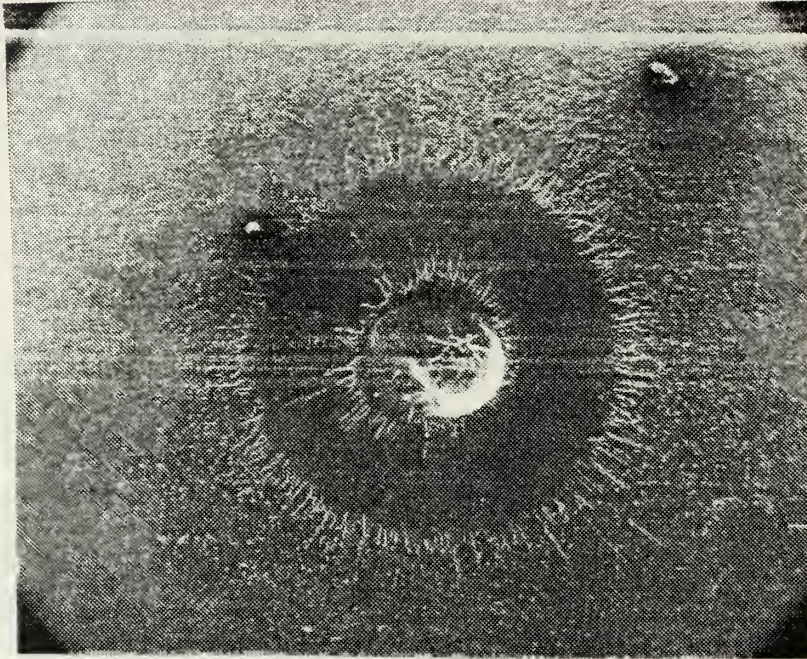


Figure 2. Stainless steel surface damaged by one 5ns, high irradiance, focused laser pulse. Magnification 28X.



Figure 3. Flow pattern 3mm from laser impact point which is to the right of figure. Magnification 700X.



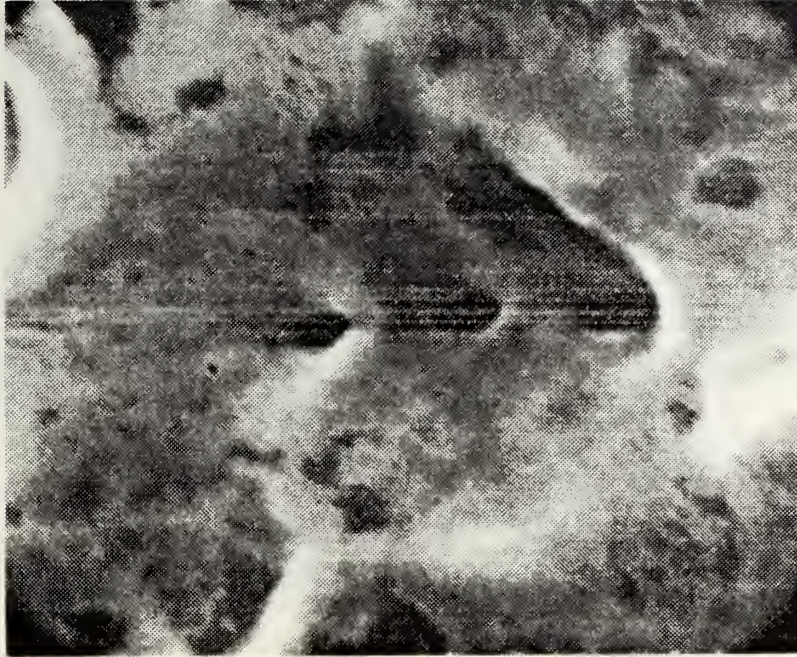


Figure 4. Three cathode craters and V-shaped flow pattern. Laser impact point is to the right. Magnification 2,800X.

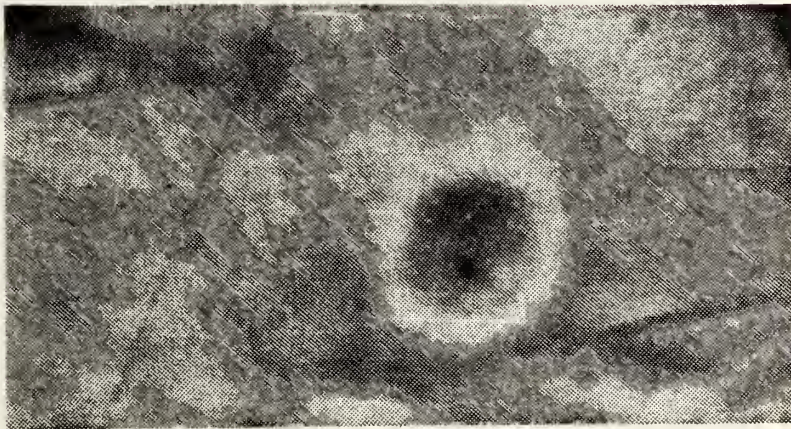


Figure 5. Unipolar arc crater near edge of target disk. Magnification 7,000X.

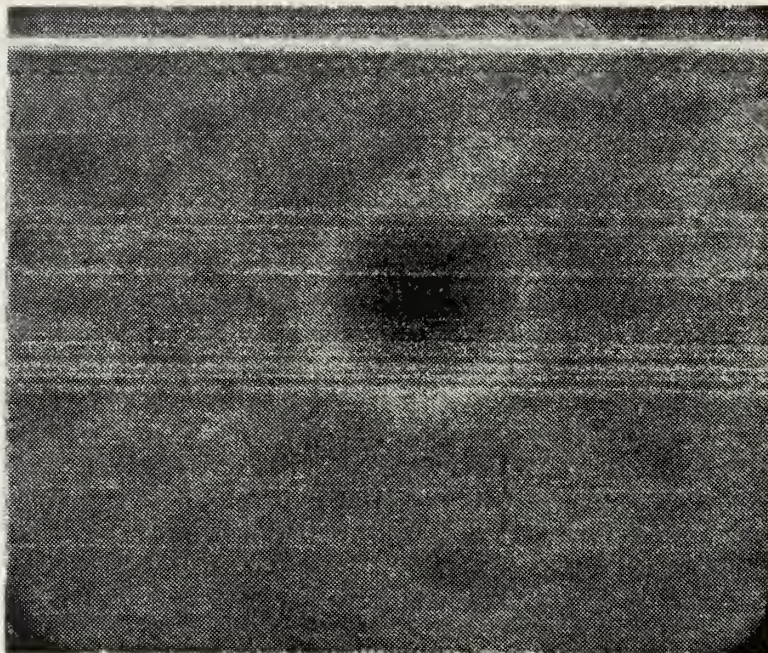


Figure 6. Cathode hole of a unipolar arc after short burntime. Magnification 14,000X.

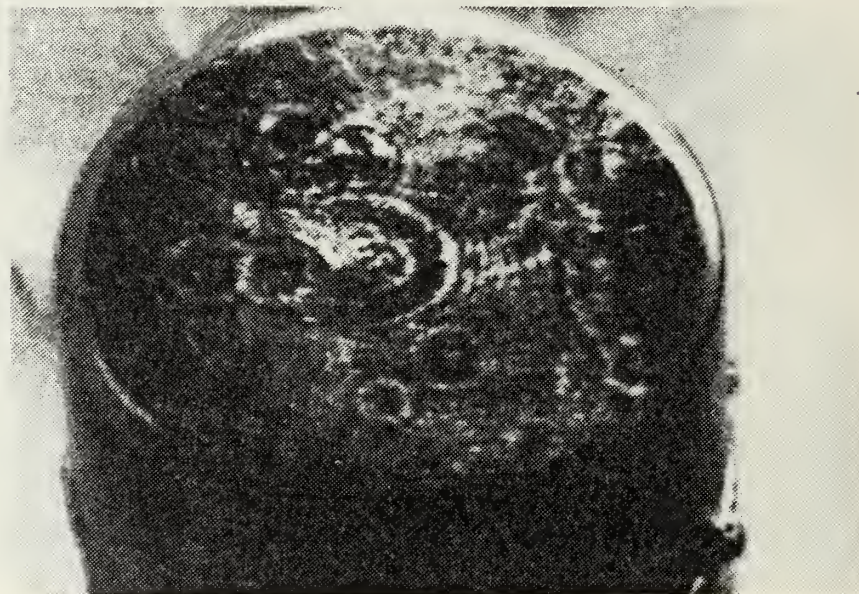


Figure 7. Burn pattern of low irradiance, defocused laser pulse on 12 mm diameter stainless steel target disk.

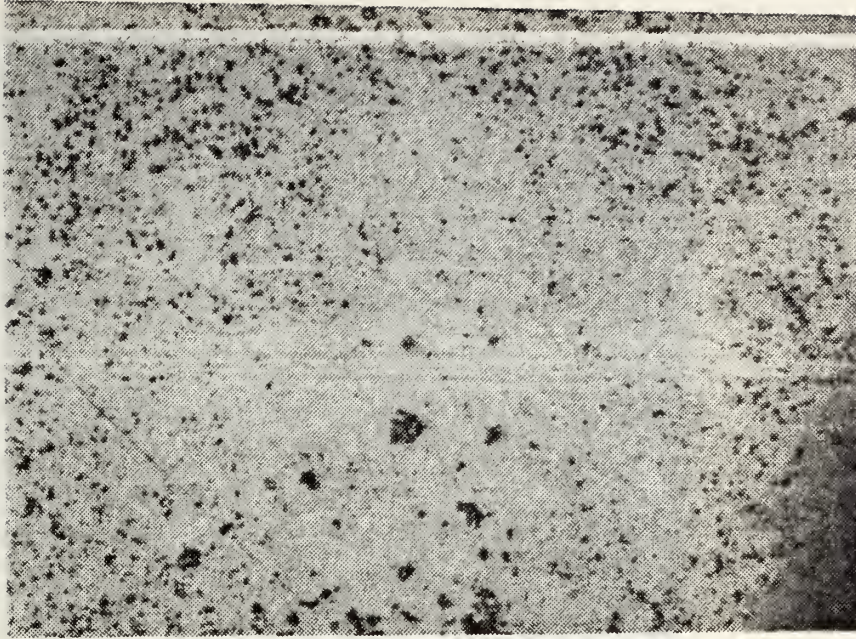


Figure 8. Enlargement (100X) with optical microscope, of an interference "ring". The "ring" consists of a variation of the surface density of unipolar arc craters.

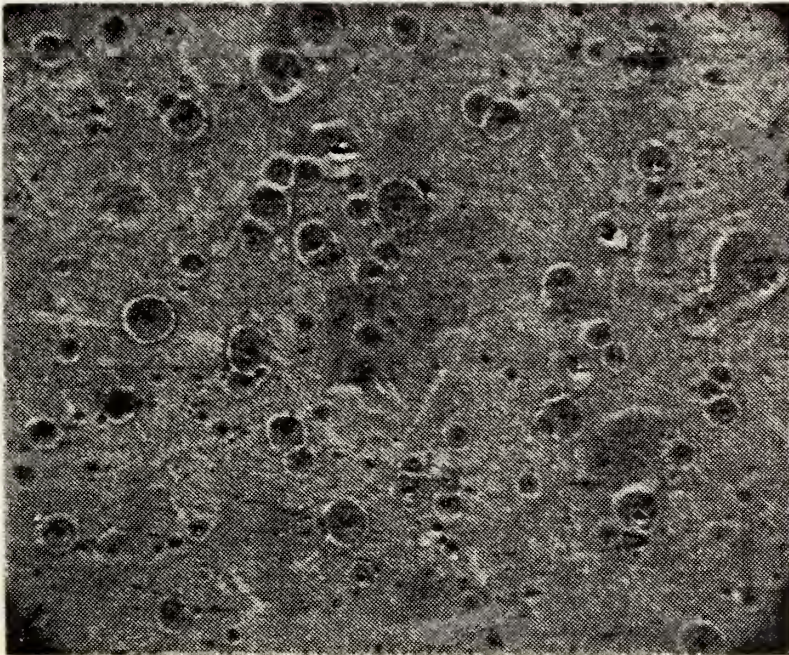


Figure 9. Further enlargement (700X with SEM) of interference "ring" shows unipolar arc craters.

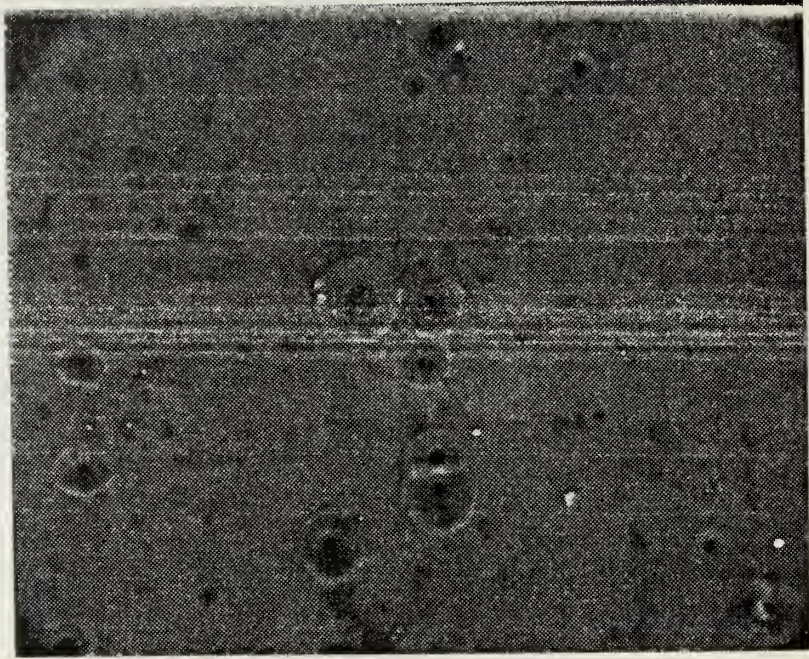


Figure 10. Burn pattern consists of unipolar arc craters of various size. SEM photo (1,400X)

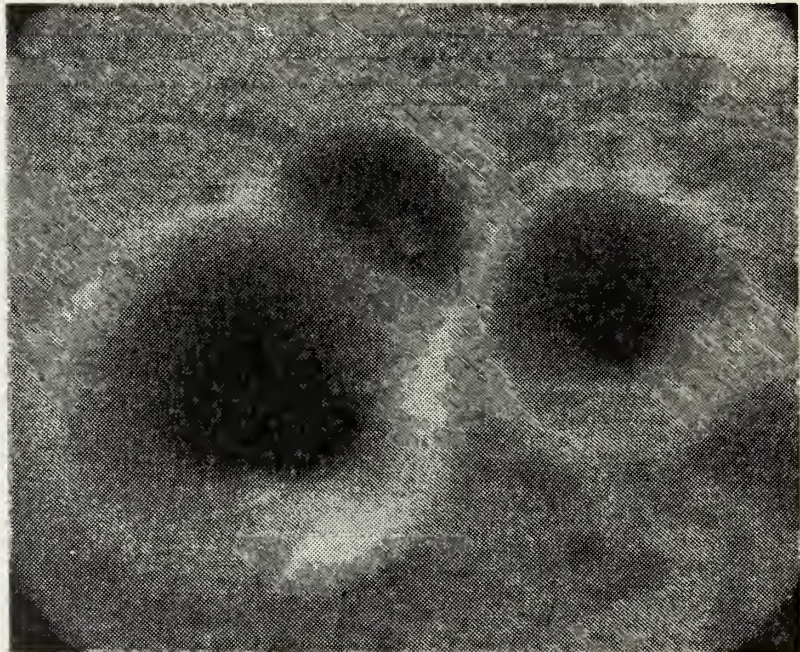


Figure 11. The diameter of small cathode holes of about  $0.7 \mu\text{m}$  is smaller than the wave length of the laser  $1.06 \mu\text{m}$ .

DISTRIBUTION LIST

	No. Copies
1. Professor Fred Schwirzke Code 61Sw Naval Postgraduate School Monterey, California 93943	40
2. Dudley Knox Library Naval Postgraduate School Monterey, California 93943	2
3. Naval Research Laboratory Washington, DC 20375	6
4. Defense Technical Information Center Attn: DTIC-DDR Cameron Station Alexandria, VA 22314	2





DUDLEY KNOX LIBRARY



3 2768 00338346 4